Fig. 3. (a) Glucose oxidation current of downstream glucose anode ($I_{glucose}$ at downstream) vs. O_2 reduction current of upstream BOD cathode (I_{O_2} at upstream), and (b) O_2 reduction current of downstream BOD electrode (I_{O_2} at downstream) vs. O_2 reduction current of upstream BOD electrode (I_{O_2} at upstream), measured in the phosphate buffer (pH 7) containing 0.1 M NaCl, 10 mM glucose and 1 mM NAD$^+$ at room temperature, with a flow rate of 0.3 mL min^{-1}. Channel height: 1 mm.

pre-reduction current (I_{O_2} at upstream). This linear relationship can be expressed as the equation,

$$i_{downstream} = i^0_{downstream} - Ni_{upstream} \tag{1}$$

where $i^0_{downstream}$ is the current at the downstream electrode when $i_{upstream} = 0$, and N is the efficiency of O_2 elimination estimated as 0.065 from the decay of the plot. The experimental N value (0.065) is unfortunately inferior to the theoretical one (Nth = 0.13) calculated by the equation for the channel flow electrode system [31], probably because of unknown factors affecting N: e.g., the thickness (several tens of μm) and roughness of the KB electrodes. The Nth is the function of only electrode configuration [31], and suggests that a higher Nth would be obtained by a narrower electrode gap and smaller
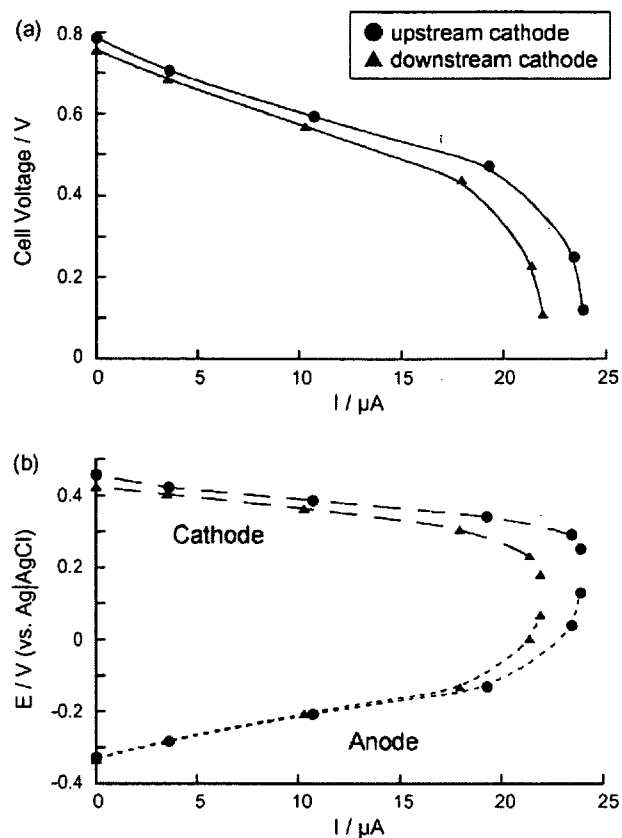
Fig. 4. (a) $V–I$ curve of microfluidic biofuel cell (—), and (b) $E–I$ curves of anode (· · ·) and cathode (- - -) operating under air-saturated phosphate buffer (pH 7) containing 0.1 M NaCl, 10 mM glucose and 1 mM NAD$^+$ at room temperature, with a flow rate of 0.3 mL min^{-1}. The cells were operated with upstream cathode (●) or downstream cathode (■). Channel height: 1 mm.

upstream cathode, while the small cathode has the disadvantage for generating larger power.

3.3. Microfluidic biofuel cell performance

By connecting enzymatic anode and cathode through external resistance, biofuel cell performance was evaluated for 0.3 mL min^{-1}. Fig. 4a shows the cell performance ($V–I$ curve) in an air-saturated solution with an open circuit voltage (V_{oc}) of around 0.8 V and maximum current (I_{max}) of over 20 μA. This is in agreement with the prediction from performance of each anode and cathode (Fig. 2). The $V–I$ curve obtained with the upstream-cathode cell (●) was bigger than that with the downstream-cathode cell (▲), especially in the higher current region. The I_{max} increased 10% by placing the cathode upstream, mainly reflecting the improved anode as judged from the analogy between the shape of the $V–I$ curve of the cell (—) and the $E–I$ curve of the anode (· · ·). The E-I curve of the cathode (- - -) was also somewhat changed, indicating the consumption of O_2 at the upstream anode by the adverse reaction with enzymes and mediators. Another separate experiment with an O_2-bubbled solution brought smaller I_{max} (ca. 20 μA) due to the larger O_2 flux to the upstream anode, which was improved 15% by pre-reduction of O_2 at the upstream cathode. These results have proven that the cell design with upstream cathode is effective in protect-
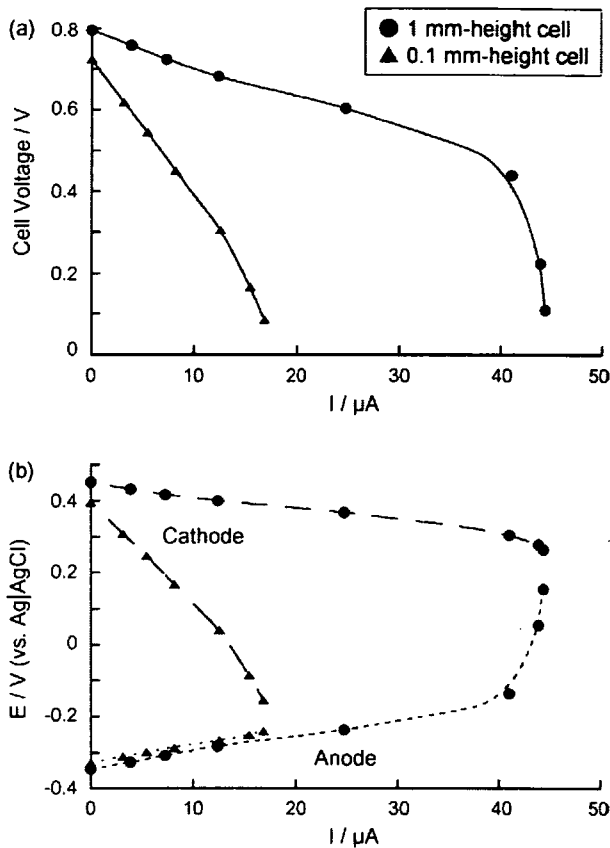
Fig. 5. (a) V–I curves of sandwich type microfluidic biofuel cell (—), and (b) E–I curves of anode (· · ·) and cathode (- - -) operating under air-saturated phosphate buffer (pH 7) containing 0.1 M NaCl, 10 mM glucose and 1 mM NAD⁺ at room temperature, with a mean flow rate of 10 cm min⁻¹. Channel height: 1 mm (●) and 0.1 mm (■).

ing the anode from the oxidative environment and consequently improving cell performance.

We also studied the performance of microfluidic biofuel cells having electrodes on both bottom and upper walls of the channel (Fig. 5). These were constructed by sandwiching a silicone rubber spacer of 0.1 mm or 1 mm thickness between two electrode-patterned glass slides. Both glass slides have a set of upstream cathode and downstream anode. The I_{max} of the 1 mm-height cell (44 μA) was almost twice that for the case of a single set of electrodes as shown in Fig. 4. This result directly corresponds to the increased electrode area. In contrast, the I_{max} of 0.1 mm-height cell (▲) composed of two sets of electrodes became rather small mainly because of depletion of O_2 in the narrower flow channel, as presumed from the degraded cathodic I–E curve. Theoretically, at the maximum diffusional flux ($c = 0$ at the electrode surface), the thickness of the diffusion boundary layer δ (cm) formed on the electrode within a tube-shaped channel is expressed as [32],

$$\delta = \frac{1}{0.67}\left(\frac{DRx}{v_0}\right)^{1/3} \tag{2}$$

where D is the diffusion coefficient ($cm^2\,s^{-1}$), R the radius of the tube, x the distance measured downstream from the leading edge of the electrode (cm) and v_0 is the maximum velocity at the

axis of the tube ($r = 0$) ($cm\,s^{-1}$). From Eq. (2), the thickness of the O_2 depletion layer under the flow condition of 10 cm min⁻¹ (0.3 mL min⁻¹) is calculated to be about several hundred μm at a position 1 mm-downstream from the leading edge of the cathode, which can fully cover the 0.1 mm-height fluidic channel and lower cell performance. On the other hand, from the viewpoint of the "volume density", the 0.1 mm-height narrower cell is superior to the 1 mm-height cell; the volume density of I_{max} and P_{max} of the 0.1 mm-height cell was 3.8 times and 2 times, respectively, as large as those of the 1 mm-height cell. The optimum efficient operation with the highest density of output would be at the flow condition forming depletion layer comparable to the channel height.

4. Conclusion

We constructed an enzyme-based microfluidic biofuel cell to study the effects of pre-electrolysis of O_2 at the upstream cathode on the performance of the downstream anode under regulated fluidic conditions. The upstream cathode successfully reduced the O_2 flux to the anode, and consequently improved the glucose oxidation performance. The maximum cell current with the upstream-cathode cell was about 10% higher than that with the downstream-cathode cell. It was experimentally demonstrated that, we need to take into account the depletion of fuel and oxidant within the channel that depends on the channel height and flow rate in addition to the electrode configuration. One of the optimum operating conditions would be when the flow forming depletion layer is comparable to the channel height. The active O_2 supply from external air through the channel wall should be effective in improving the cell performance. In such an O_2-concentrated condition, the cell construction with upstream cathode would become more significant to maintain anode's performance.

References

[1] K.B. Lee, J. Micromech. Microeng. 15 (2005) S210–S214.
[2] K.B. Lee, L.W. Lin, J. Microelectromech. Syst. 12 (2003) 840–847.
[3] R.S. Jayashree, L. Gancs, E.R. Choban, A. Primak, D. Natarajan, L.J. Markoski, P.J.A. Kenis, J. Am. Chem. Soc. 127 (2005) 16758–16759.
[4] E.R. Choban, L.J. Markoski, A. Wieckowski, P.J.A. Kenis, J. Power Sources 128 (2004) 54–60.
[5] R. Ferrigno, A.D. Stroock, T.D. Clark, M. Mayer, G.M. Whitesides, J. Am. Chem. Soc. 124 (2002) 12930–12931.
[6] M. Togo, A. Takamura, T. Asai, H. Kaji, M. Nishizawa, Electrochim. Acta 52 (2007) 4669–4674.
[7] K.G. Lim, G.T.R. Palmore, Biosens. Bioelectron. 22 (2007) 941–947.
[8] Y. Kamitaka, S. Tsujimura, N. Setoyama, T. Kajino, K. Kano, PCCP Phys. Chem. Chem. Phys. 9 (2007) 1793–1801.
[9] F. Sato, M. Togo, M.K. Islam, T. Matsue, J. Kosuge, N. Fukasaku, S. Kurosawa, M. Nishizawa, Electrochem. Commun. 7 (2005) 643–647.
[10] C.M. Moore, S.D. Minteer, R.S. Martin, Lab Chip 5 (2005) 218–225.

[11] A. Heller, AiChE J. 51 (2005) 1054–1066.
[12] A. Heller, PCCP Phys. Chem. Chem. Phys. 6 (2004) 209–216.
[13] S.C. Barton, J. Gallaway, P. Atanassov, Chem. Rev. 104 (2004) 4867–4886.
[14] N. Mano, F. Mao, W. Shin, T. Chen, A. Heller, Chem. Commun. (2003) 518–519.
[15] S. Tsujimura, K. Kano, T. Ikeda, Electrochemistry 70 (2002) 940–942.
[16] N. Mano, F. Mao, A. Heller, J. Am. Chem. Soc. 124 (2002) 12962–12963.
[17] S. Tsujimura, M. Fujita, H. Tatsumi, K. Kano, T. Ikeda, PCCP Phys. Chem. Chem. Phys. 3 (2001) 1331–1335.
[18] E. Katz, A.F. Buckmann, I. Willner, J. Am. Chem. Soc. 123 (2001) 10752–10753.
[19] T. Chen, S.C. Barton, G. Binyamin, Z.Q. Gao, Y.C. Zhang, H.H. Kim, A. Heller, J. Am. Chem. Soc. 123 (2001) 8630–8631.
[20] G.T.R. Palmore, H. Bertschy, S.H. Bergens, G.M. Whitesides, J. Electroanal. Chem. 443 (1998) 155–161.
[21] T. Tamaki, T. Ito, T. Yamaguchi, J. Phys. Chem. B 111 (2007) 10312–10319.
[22] N. Mano, F. Mao, A. Heller, J. Electroanal. Chem. 574 (2005) 347–357.
[23] N. Mano, A. Heller, Anal. Chem. 77 (2005) 729–732.
[24] N. Mano, F. Mao, A. Heller, J. Am. Chem. Soc. 125 (2003) 6588–6594.
[25] H.H. Kim, N. Mano, X.C. Zhang, A. Heller, J. Electrochem. Soc. 150 (2003) A209–A213.
[26] H. Tatsumi, H. Nakase, K. Kano, T. Ikeda, J. Electroanal. Chem. 443 (1998) 236–242.
[27] S. Tsujimura, K. Kano, T. Ikeda, J. Electroanal. Chem. 576 (2005) 113–120.
[28] S. Tsujimura, T. Nakagawa, K. Kano, T. Ikeda, Electrochemistry 72 (2004) 437–439.
[29] Y. Kamitaka, S. Tsujimura, K. Kataoka, T. Sakurai, T. Ikeda, K. Kano, J. Electroanal. Chem. 601 (2007) 119–124.
[30] M. Tominaga, M. Otani, M. Kishikawa, I. Taniguchi, Chem. Lett. 35 (2006) 1174–1175.
[31] T. Tsuru, Mater. Sci. Eng. A: Struct. Mater. Prop. Microstruct. Process. 146 (1991) 1–14.
[32] V.G. Levich, Physicochemical Hydrodynamics, Prentice-Hall, Inc., Englewood Cliffs, NJ, 1962.